RESEARCH ARTICLE

Macromolecular Materials and Engineering
www.mame-journal.de

Smart Shape Memory Polyurethane with Photochromism and Mechanochromism Properties

*Xiaofei Wang, Yang He, and Jinsong Leng**

The combination of shape memory effects and multi-functionalities in smart materials is becoming one of the hottest research directions in the field of actuators and robotics. In this study, *N*-hydroxyethyl-3,3-dimethyl-6-nitroindoline spiropyran (SP) is chemically grafted into a polyurethane matrix to prepare ultraviolet light-actuated shape memory thermoplastic polyurethane, which first integrates three unique properties including shape memory, photochromism, and mechanochromism. The FTIR, WAXD, SAXS, DSC, TGA, and shape memory tests reveal that the shape memory transformation temperature of 4.6 wt% SP-based shape memory polyurethane is 41.2 °C, and it has the highest shape memory performance, as indicated by shape fixation and shape recovery ratios of 97.4% and 93.7%, respectively. Furthermore, "bionic fingers" with diversely selective actuation properties are fabricated, which exhibit a series of programmable multi-segment motions to meet potential applications in the field of soft actuators.

1. Introduction

Shape memory polymer (SMP) is an intelligent material that can adjust its state parameters (such as shape, position, and strain) under external stimulation, to return to the preset state and is widely used in aerospace, biomedicine, soft actuators, and other fields.[1–9] There are several types of SMP materials, and they can be divided into thermally, electrically, photo, magnetically, and chemically actuated SMPs.[10–28] At present, most SMPs are thermally actuated, and they are heated to a shape memory transition temperature T_{trans} (T_{trans} is the shape memory transition temperature, which is the glass transition temperature or melting transition temperature). Then, the temporary shape of the SMP is fixed by maintaining the external force and reducing the temperature to below T_{trans}. Finally, the SMP returns to its original shape when it is heated to temperatures above T_{trans}.[29] Shape memory polyurethane (SMPU) has the advantages of low price, adjustable hard and soft segments, no by-products, good wear resistance, and high mechanical strength. However, in some applications, such as biomedical engineering, excessive temperature causes irreversible damage to biological tissues; thus, thermal actuation is not a good stimulation source. There is an urgent need to develop new SMPs to meet the needs of different fields.

Photo-actuated SMPs have the unique advantages of non-contact, fixed-point, fast response, and precise control deformation. In addition, they can directly convert light energy into mechanical energy and improve the efficiency of light utilization.[30–35] Therefore, researchers have focused on the photo actuation SMP. Lendlein et al. were the first to graft cinnamic acid (CA) to acrylate copolymer networks using the radical copolymerization method to fabricate a photo-actuated SMP thin film. When the film was irradiated with a wavelength greater than 260 nm, two CA molecules had cross-linking reaction, and the temporary shape was fixed simultaneously. When the wavelength was less than 260 nm, the CA dimer was destroyed and underwent a de-crosslinking reaction, and the thin film returned to its original state.[36] In 2019, Zhang et al. doped 4-cyano-4'-pentyloxyazobenzene (5CAZ) and up-conversion luminescent nanoparticles (UCNPs) ($NaYF_4$: Yb 25 mol%, Er 2 mol% @ $NaYF_4$: Nd 30 mol%, and core–shell UCNPs with an average particle diameter of ≈20 nm) into a SMPU matrix to produce ultraviolet light (UV), visible light, and near-infrared (NIR) light-responsive SMP composites. Among them, 5CAZ, as azobenzene molecules, served as a "photo-switch" and underwent trans-cis and cis-trans photoisomerization upon UV and visible light irradiation, respectively, and, UCNPs could convert 808 nm NIR light into green fluorescence by continuous photon absorption.[37–39]

At present, most photo-actuated SMPs rely on the photochemical reaction of CA groups or azobenzene groups or the photothermal effect of photothermal nanoparticles such as graphene oxide.[40–42] However, there are few reports on the photoplasticization effect to actuate shape deformation. By consulting relevant literature, it was discovered that spiropyran (SP) compounds not only have the characteristics of a photochromic effect but also have a photoplasticization effect.[43,44] When irradiated with UV light, the C–O bond of the SP molecules was broken, resulting in isomerization and rearrangement of the molecular structure and electron configuration, and ring-opened structures were formed. These ring-opened structures weakened the interaction force of the polymer molecular chains; thus, the molecular

X. Wang, Y. He, J. Leng
Center for Composite Materials and Structures
Harbin Institute of Technology
Harbin 150080, P. R. China
E-mail: lengjs@hit.edu.cn

The ORCID identification number(s) for the author(s) of this article can be found under https://doi.org/10.1002/mame.202100778

DOI: 10.1002/mame.202100778

chains of the soft segments became soft and moved faster, facilitating the restoration of the SMP from a temporary shape to the original shape. Meanwhile, the polymer turned purple. Thereafter, through heating or visible light irradiation, SP molecules changed from ring-opened structures to ring-closed structures, and the polymer returned to its original color.[45,46] In addition, SP has a mechanochromic effect, which has a molecular structure transition from the ring-closed to the ring-opened upon external force. This force can be tensile stress, mechanical grinding force, or isotropic hydrostatic pressure. Therefore, it has the potential for mechanochemical sensing and damage warning applications.[47–49]

In this study, first, a SP molecule with a photoplasticization effect was chemically grafted into a polyurethane matrix (diphenylmethane diisocyanate (MDI) was used as the hard segment, whereas polytetrahydrofuran dialcohol (PTMEG) was used as the soft segment) to fabricate UV light-actuated shape memory thermoplastic polyurethane (SMTPU-SP), addressing the problems of physical fabrication methods, such as uneven dispersion, stress concentration, and aggregate crystallization. Second, photochromic and mechanochromic effects of the prepared SMTPU-SP were studied to verify their potential applications in stress sensors and anti-counterfeiting engineering. Third, the 365 nm UV actuated SMTPU-SP was flexibly assembled with SMTPU under 808 nm NIR light actuation and thermo-responsive SMTPU to obtain "bionic fingers" with multi-selective actuation and multi-segment motions, which could be utilized in programmable soft actuator areas.

2. Results and Discussion

2.1. Molecular Structure of SMTPU-SP

The FTIR spectra of the preparation process of SMTPU-SP are shown in **Figure 1**a and Scheme S1 (Supporting Information). In the PTMEG-MDI-BD spectrum, 2240 cm^{-1} was the –NCO characteristic absorption peak. In the SP spectrum, 3350 cm^{-1} was the –OH characteristic absorption peak, and in the SMTPU-SP spectrum, 3280 cm^{-1} was the carbamate's –NH absorption peak. The –NCO absorption peak in the PTMEG-MDI-BD spectrum and the hydroxyl group characteristic absorption peak in the SP spectrum both disappeared in the SMTPU-SP spectrum; meanwhile, the –NH absorption peak (3280 cm^{-1}) of the carbamate appeared in the SMTPU-SP spectrum, indicating that PTMEG-MDI-BD reacted with SP and formed SMTPU-SP. The FTIR test demonstrated that the SP compound was grafted into the polyurethane matrix successfully.

Figure 1b shows the ^1H NMR spectrum of SMTPU-SP, where the chemical shift at δ = 7.283 ppm is the characteristic peak of hydrogen on the benzene ring, that at δ = 3.437 ppm is the characteristic peak of CH_2 associated with PTMEG and carbamate, that at δ = 1.574–1.642 ppm is the characteristic peak of –CH_2 associated with 1,4-butanediol and carbamate, and that at δ = 1.287 ppm is the characteristic peak of –CH_3 on the SP molecule, confirming the successful preparation of the spiropyran-grafted-polyurethane polymer.

Figure 1c shows the UV–vis curves of the SMTPU-SP-2.4 thin film before and after UV irradiation, and we utilized the sample to demonstrate the molecular structure changes of the SP under UV light irradiation. The ring-closed structure of SP was a vertical conformation molecule, which had no absorption in the visible light zone. When the ring-opened structure of the SP formed a planar conjugated structure after UV light irradiation, it exhibited strong absorption in the visible light region. The UV–vis absorption spectrum was used to characterize the state of the SP in the polymer. It can be observed from Figure 1c that an absorption peak of SMTPU-SP-2.4 appeared at 558 nm after UV exposure, which was the same as that reported in the reference, indicating that the polymer had undergone structural change from a ring-closed structure to a ring-opened structure upon UV light irradiation.[43,44] Taking SMTPU-SP-1.2 as an example, we tested the UV–vis curves of the sample before and after the mechanochromic effect. As shown in Figure 1d, the absorption peak of SMTPU-SP-1.2 appeared at 561 nm after stress, indicating that the polymer had undergone a molecular structure change from a ring-closed structure to a ring-opened structure upon stress, and had a mechanochromic effect.

Figure 1e shows the WAXD spectrum of SMTPU-SP before 365 nm UV light irradiation. It can be seen from Figure 1e that 2θ had a broad peak at ≈20° because there was a large number of amorphous, microcrystalline, or semicrystalline structures in the SMTPU-SP system. In the polyurethane system, 2θ = 19.34° and 20.34° were the crystallization peaks of the soft segment PTMEG, of which 2θ = 19.34° corresponded to the 110 crystalline face, whereas 2θ = 20.34° corresponded to the 200 crystalline face. This revealed that there were some ordered sequences in the system, and as the content of the SP increased, the diffraction peak intensity of the system first increased and thereafter decreased, indicating that the crystallinity of the system first increased and thereafter decreased. When the SP content was 2.4 wt%, the SMTPU-SP system had the highest crystallinity. Figure 1f–h shows the WAXD comparison spectrum of SMTPU-SP before and after UV irradiation. The positions of the diffraction patterns and intensity of the soft segment PTMEG in Figure 1f were almost the same before and after UV light irradiation, indicating that the SP content of 1.2 wt% had no significant effect on the SMTPU-SP system. In Figure 1g,h, the positions of the diffraction peaks and intensities of the soft segments changed after UV light irradiation. The peak at 2θ = 19.34°(110 crystal face) was shifted to 19.27° for the SMTPU-SP-2.4 sample after UV light irradiation, and shifted to 19.17° for the SMTPU-SP-4.6 sample after UV light irradiation. The diffraction peak displacement and intensity of the diffraction peak increased with increasing SP content, proving that the photoplasticization effect of the SMTPU-SP was enhanced. After the SMTPU-SP was irradiated with UV light, the SP molecule underwent photoisomerization, such that the orthogonal ring-closed structure was transformed into a planar ring-opened structure. These ring-opened structures weakened the interaction force of the SMTPU-SP molecular chain segments, accelerating the short-range motion of the polymer chain segments and causing the peak position of the soft segment to change.

SAXS was used to characterize the microphase separation structure of the SMTPU-SP. The long period of the SMTPU-SP corresponds to the total thickness of the soft and hard segments. **Figure 2**a–e shows the SAXS two-dimensional (2D) scattergram of the SMTPU-SP, and Figure 2f shows the one-dimensional scattergram converted from the 2D scattergram processed by RAW

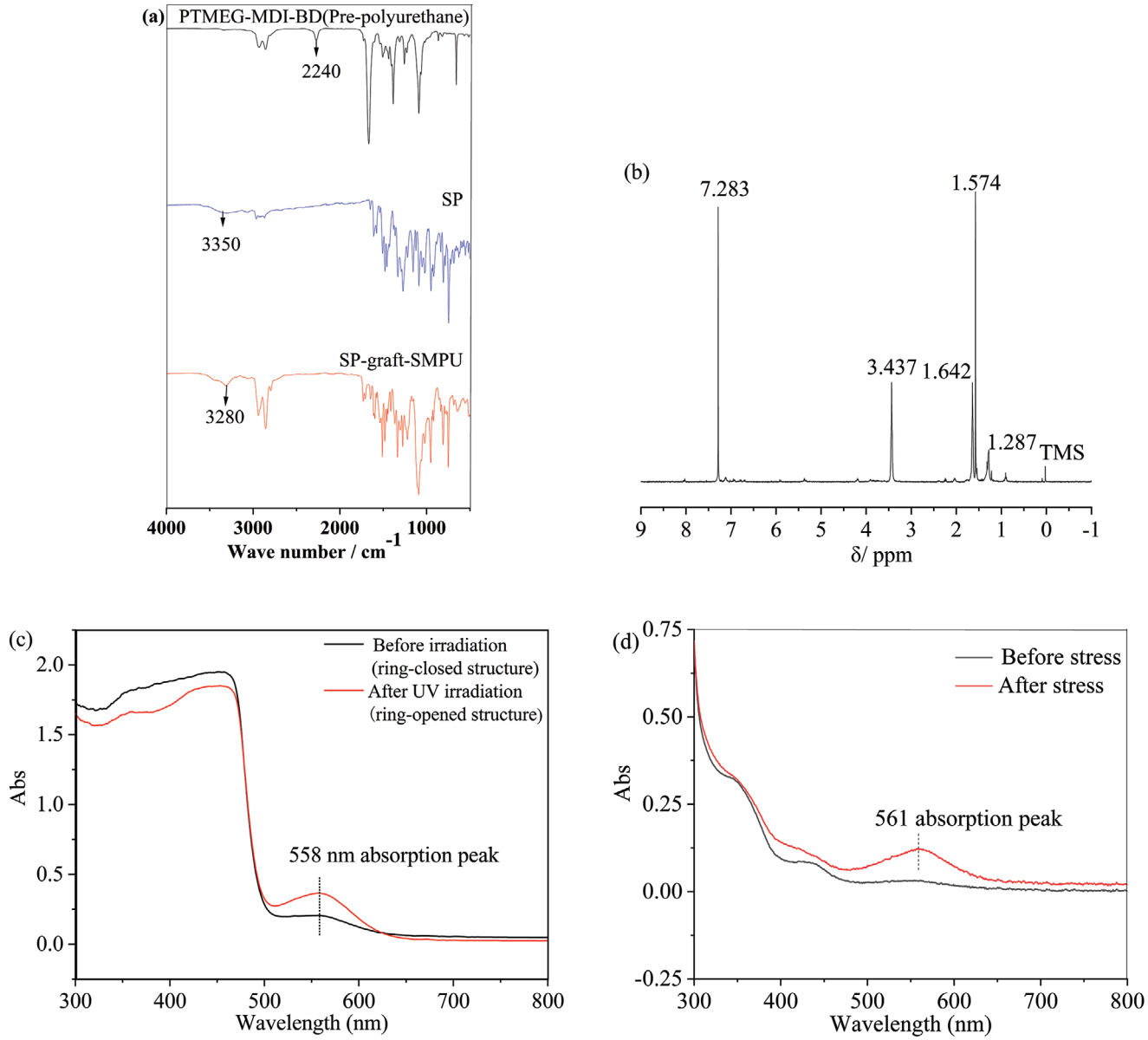

Figure 1. a) FTIR spectrum of the preparation process of SMTPU-SP, b) ^{1}H NMR of SMTPU-SP, c) UV–vis curve of SMTPU-SP-2.4 before and after 365 nm UV light irradiation, d) UV–vis curve of SMTPU-SP-1.2 before and after stress, e) WAXD spectrum of SMTPU-SP (before 365 nm UV light irradiation), f–h) WAXD spectrum of SMTPU-SP (before and after 365 nm UV light irradiation).

software. As shown in Figure 2f, the maximum value of the scattering vector (q_{max}) of SMTPU-SP-0 was 0.2657 nm^{-1}, and according to the long period calculation equation $L = 2\pi/q_{max}$, the long period of SMTPU-SP-0 was 23.48 nm. The q_{max} of SMTPU-SP-4.6 was 0.2656 nm^{-1}, and the long period was 23.66 nm. The slight change may be because the SP was grafted into the polyurethane and changed the molecular chain segment aggregates.

2.2. Thermodynamic Properties of SMTPU-SP

The shape memory transformation temperature of SMTPU-SP was investigated using DSC. As shown in Figure 2g, the melting endothermic peak appeared in the temperature range of 29–43 °C; thus, the soft segment had crystal melting within that temperature range. The melting point of soft segments PTMEG of SMTPU-SP-0, SMTPU-SP-1.2, SMTPU-SP-2.4, SMTPU-SP-3.5, and SMTPU-SP-4.6 were 29.7, 32.0, 42.3, 42.2, and 41.2 °C, respectively. As the content of SP increased, the melting point of the soft segment first increased and thereafter decreased, and SMTPU-SP-2.4 had the highest melting point temperature, up to 42.3 °C. This is because SP was chemically grafted into the polyurethane molecular chains. The SP had rigid groups such as benzene rings. As the content increased, the rigidity of the polyurethane molecular chain increased, and the melting point of the soft segment increased; however, as the content increased,

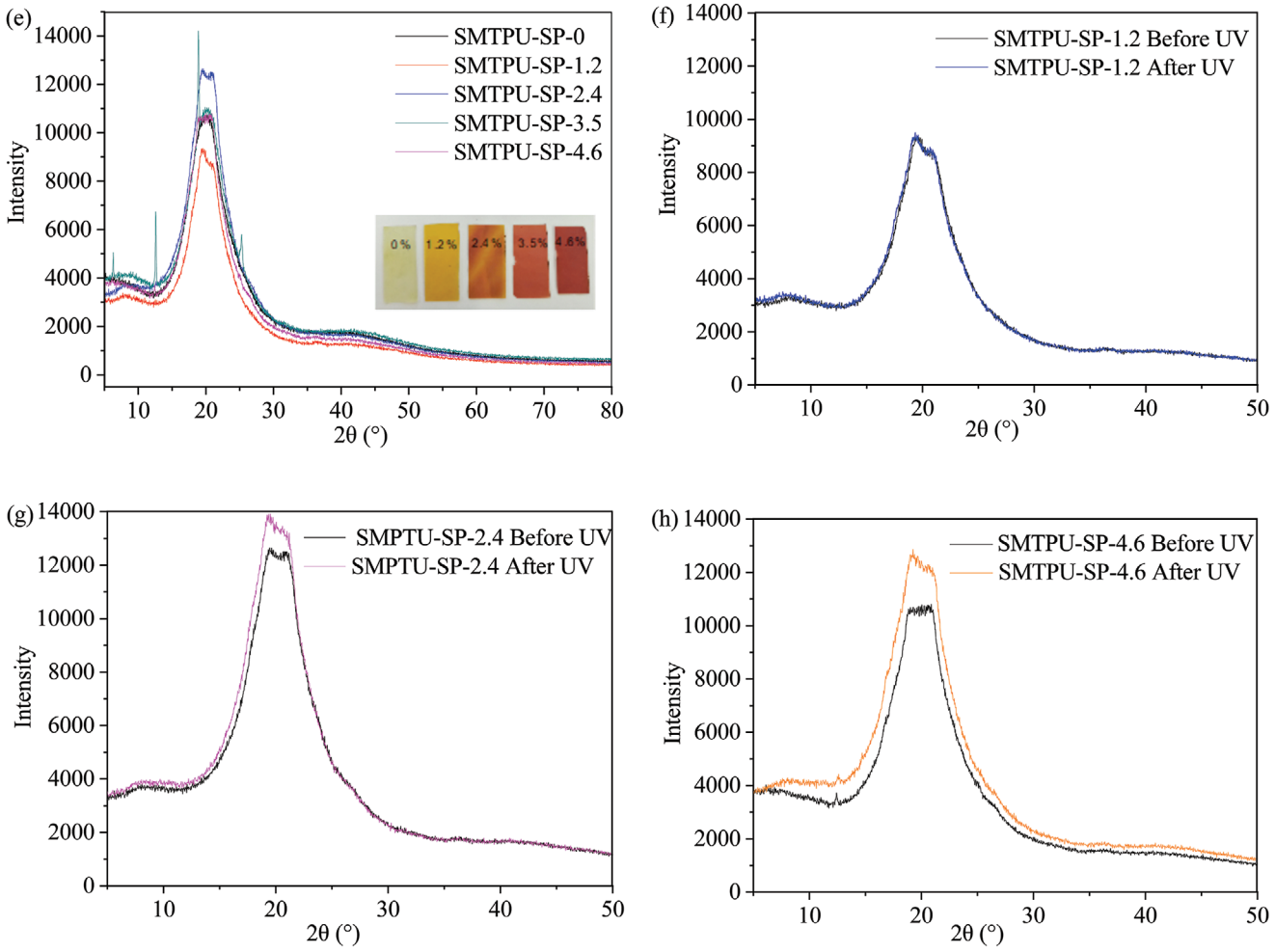

Figure 1. *Continued*

the structural regularity of the molecular chain of the polymer was destroyed and the crystallization of the soft segment was adversely affected, causing the melting point of the soft segment to drop again.

Polyurethane crystallization is important for the shape memory effect. On one hand, crystallization is equivalent to the physical cross-linking points, which can prevent the segment from slipping during the stretching process. On the other hand, as the crystallinity of the soft segment phase increases, the stored internal stress also increases during the shape deformation process, which is conducive to shape recovery. The critical temperature of the polymer is ≈29–43 °C, and the crystal zone of the soft segment melts above the T_{trans}, which makes the molecular chain move easily, and it deforms upon external stress. If the deformed polyurethane is cooled to 0 °C, the temporary shape can be fixed. Thus, in the shape memory process, the thermodynamic phase transition of the soft segment is of great significance for fixing the temporary shape.

The thermal stability of SMTPU-SP was characterized by TGA. Figure 2h,i shows the TG and DTG curves of SMTPU-SP, respectively. The DTG curve was obtained by first-order derivation of the TG curve. The peak in the DTG curve represents the decomposition rate of the polymer at this temperature. The peak is clearer, and the decomposition rate is faster. As shown in Figure 2h, the curve was flat below 200 °C, indicating that the weight loss was very small, and there was hardly any decomposition in the polymer. In the range of 300–500 °C, the polymer underwent rapid decomposition, and when the temperature reached 500 °C, the polymer was almost completely decomposed. In Figure 2h, the 5% decomposition temperature of SMTPU-SP-0, SMTPU-SP-1.2, SMTPU-SP-2.4, SMTPU-SP-3.5, and SMTPU-SP-4.6 were 271.8, 225.3, 279.8, 250.3, and 259.0 °C, respectively. On the DTG curves, the peak position was the maximum decomposition rate temperature ($T_{dec,\ max}$) of the material, and the $T_{dec,\ max}$ of SMTPU-SP-0, SMTPU-SP-1.2, SMTPU-SP-2.4, SMTPU-SP-3.5, and SMTPU-SP-4.6 were 413.4, 412.2, 411.6, 412.2, and 410.9 °C, respectively. Therefore, as the SP content increased, the thermal stability of SMTPU-SP exhibited a downward trend. This was because the SP contained rigid groups such as benzene rings, which destroyed the structural regularity of the polymer molecular chains and reduced the crystallization performance and thermal stability.

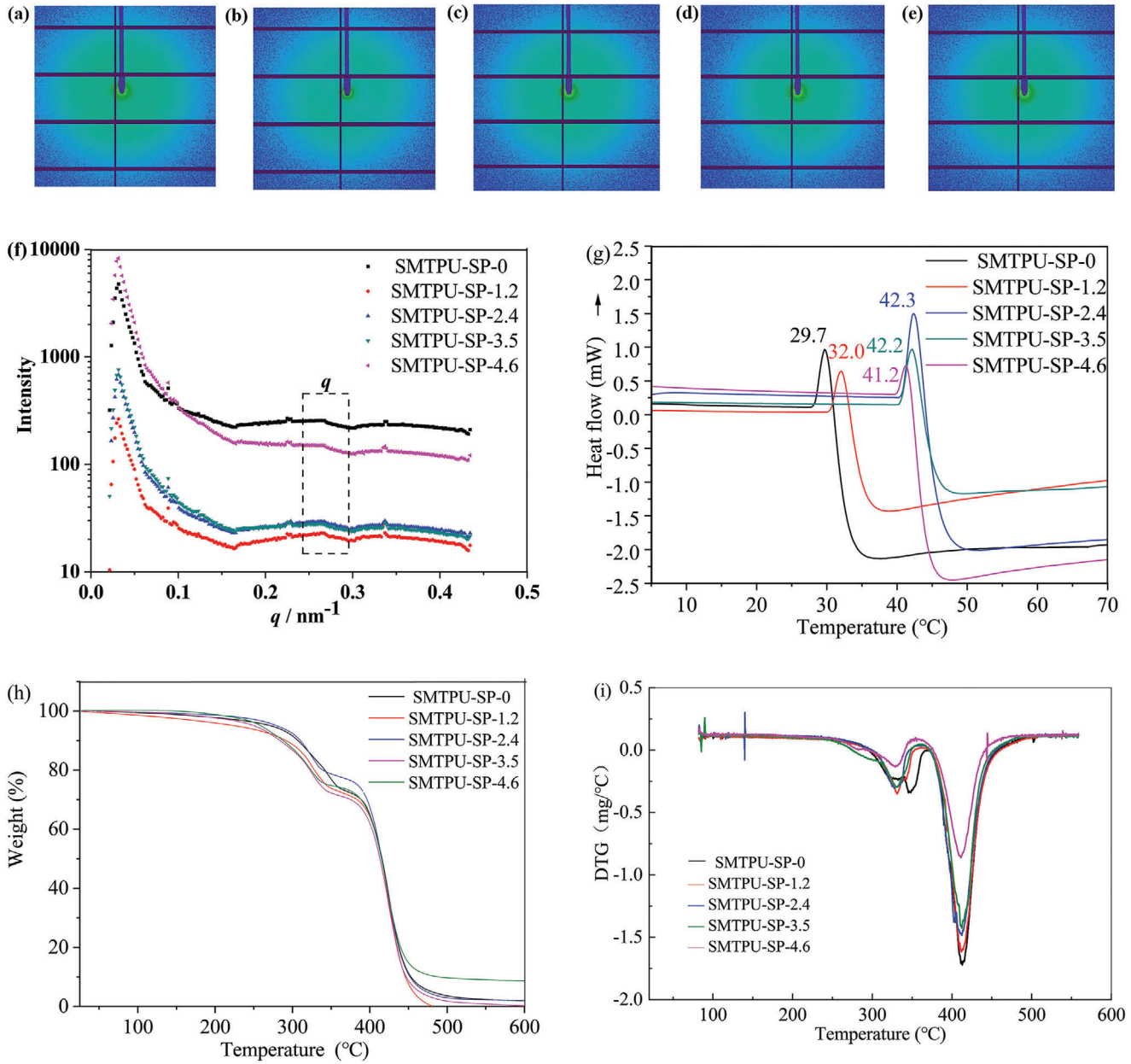

Figure 2. a–e) Two-dimensional SAXS diagram of SMTPU-SP; SMTPU-SP-0, SMTPU-SP-1.2, SMTPU-SP-2.4, SMTPU-SP-3.5, and SMTPU-SP-4.6, respectively, f) one-dimensional SAXS diagram of SMTPU-SP, g) DSC curves of SMTPU-SP, h) TG curves of SMTPU-SP, and i) DTG curves of SMTPU-SP.

2.3. Photochromic and Mechanochromic Effects

In **Figure 3**a, taking SMTPU-SP-4.6 as an example, after 365 nm UV light irradiation, the color of the sample changed from orange to purple, and through heating or visible light irradiation, the sample returned to orange. Figure 3b shows photographs of SMTPU-SP-0, SMTPU-SP-1.2, SMTPU-SP-2.4, and SMTPU-SP-4.6 after the tensile test. Pure polyurethane (SMTPU-SP-0) exhibited no color change, whereas SMTPU-SP turned purple. Figure 3a,b shows that SMTPU-SP not only had a photochromic effect but also had a mechanochromic effect. Figure 3c shows the mechanochromic behavior of the SMTPU-SP-1.2 sample. As the strain ratio increased, the color of the thin film changed from pale yellow to pale purple, and after failure, it turned purple. To quantitatively describe the colors in the photos, Adobe Photoshop CC 2017 software was used to extract the RGB color intensity. Among them, $rRC = R/(R+G+B)$, $rGC = G/(R+G+B)$,and $rBC = B/(R+G+B)$; rRC, rGC, and rBC represent the red, green, and blue components of the RGB ratio; and R, G, and B denote the average intensities of the red, green, and blue channels in the region of interest, respectively.[50] Because SMTPU-SP-1.2 mainly changed into purple under stretching conditions, we selected the rBC data for analysis, as shown in Figure 3d. When the tensile strain was 25%, there was a color transition point, indicating

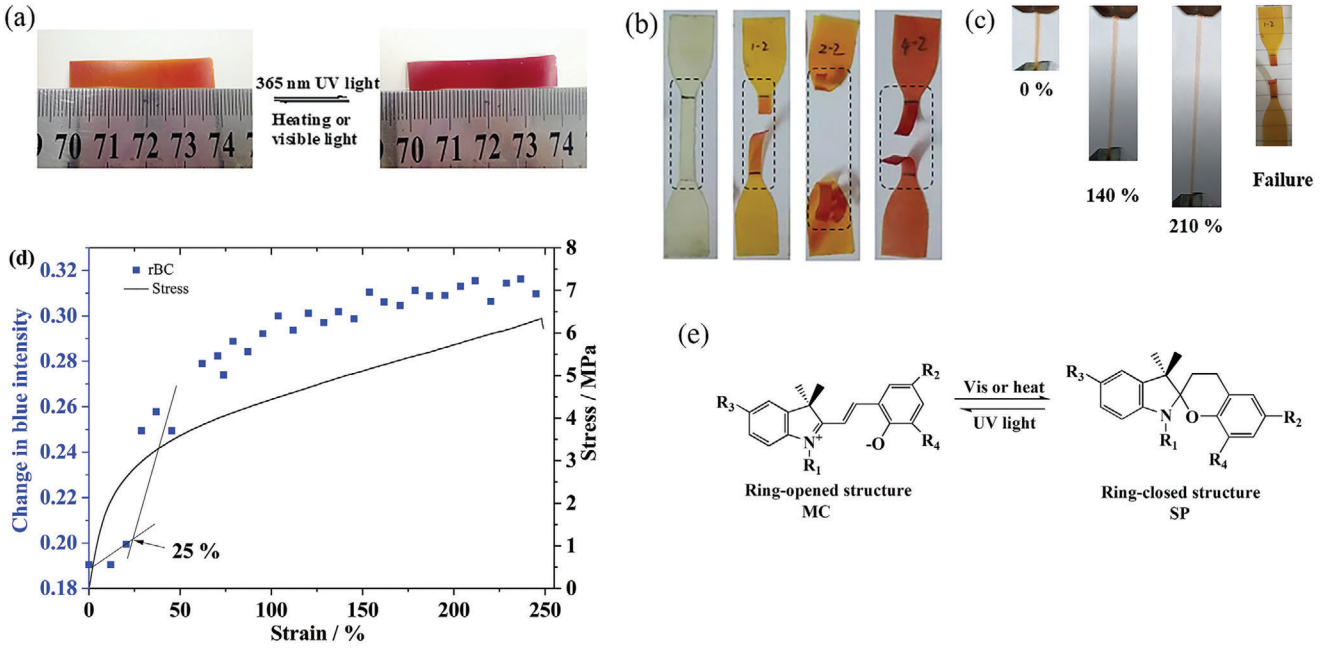

Figure 3. a) Photos of SMTPU-SP-4.6 photochromic effect process, b) photos of the SMTPU-SP mechanochromic effect; from left to right, SMTPU-SP-0, SMTPU-SP-1.2, SMTPU-SP-2.4, and SMTPU-SP-4.6, respectively, c) optical images of SMTPU-SP-1.2 during tensile test, d) stress–strain curve of SMTPU-SP-1.2 and change of blue intensity as a function of strain–strain rate of 200 (mm min^{-1}), e) mechanism of photochromic and mechanochromic effects of SMTPU-SP.

Table 1. Photochromic, photochromic recovery, and shape recovery times of SMTPU-SP.

Sample	Photochromic saturation time [s]	Photochromic recovery time [s]	Photoplasticization-induced shape recovery time [s]
SMTPU-SP-1.2	11	50	116
SMTPU-SP-2.4	13	120	82
SMTPU-SP-3.5	18	240	50
SMTPU-SP-4.6	21	360	30

that the SP structure began to change at this point, and thus the color changed. The tensile strain was not transmitted to the SP molecule at the beginning, but was consumed during the elongation and untangling deformation of the molecular chains. When the strain reached 25%, the strain on the polyurethane chain was transmitted to the SP molecule, such that the SP structure was changed, and the color also changed. As the strain increased, an increasing number of SP structures were transformed into MC structures, resulting in the rapid growth of *rBC*. After the tensile strain reached 200%, the change in *rBC* tended to be flat, indicating that almost all SP structures were converted to MC structures.

We also tested the photochromic saturation time of the SMTPU-SP upon 365 nm UV light irradiation (1.5 mW cm^{-2}) and the photochromic recovery time upon visible light irradiation (1.5 mW cm^{-2}) to determine the ring-opened and ring-closed structure transition rate. The results are summarized in **Table 1**. Under 365 nm UV light irradiation, the photochromic saturation time of the SMTPU-SP increased with increasing SP content, but the gap was not very clear. Upon visible light irradiation, the photochromic recovery time of the SMTPU-SP had a large gap, and SMTPU-SP-4.6 had the longest recovery time of 360 s. In the ring-opened structure of SP, the two aromatic rings were in a coplanar state (SP^2 hybridization), whereas in the ring-closed structure, two aromatic rings were in an orthogonal state (SP^3 hybridization). The SP^3 hybridization process needed to occupy more space and took more time; thus, more time was required to recover the original color.

Figure 3e shows the mechanism of photochromic and mechanochromic effects. After UV light irradiation, the SP is converted from a ring-closed structure to a ring-opened structure, and the ring-opened structure is a partial cyanine structure (MC); thus, the polymer turns purple. Through heating or visible light irradiation, the SP returned to the ring-closed structure, and the polymer became orange again. Similarly, under the action of tensile stress, the SP molecule changes from a ring-closed structure to a ring-opened structure , and the color also changes. Thus, SMTPU-SP has a mechanochromic effect and will be useful in visualizing stress/strain sensing and damage warning in polymer materials.

2.4. Shape Memory Effect and Programmable Soft Actuators

As shown in **Figure 4**a, taking SMTPU-SP-4.6 as an example, the sample recovered to its original shape after 365 nm UV light irradiation for 30 s. The shape memory process was as follows: The sample was heated to 60 °C for 10 min to melt the crystal zone of the soft segment. Then, it was bent in half under external force and quickly cooled to 0 °C for 10 min, after

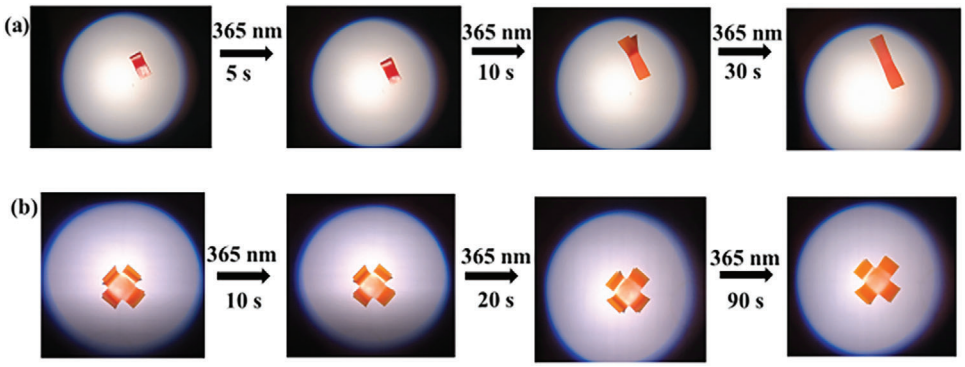

Figure 4. a) Photos of SMTPU-SP-4.6 shape recovery process, b) photos of UV-actuated unfolding process of the "box."

Table 2. Quantitative test results of shape memory properties.

Sample name	Shape fixation ratio [%]	Shape recovery ratio [%]
SMTPU-SP-0	100	0
SMTPU-SP-1.2	95.9	84.3
SMTPU-SP-2.4	99.5	90.4
SMTPU-SP-3.5	98.0	90.5
SMTPU-SP-4.6	97.4	93.7

which the external force was removed and the temporary shape was fixed. At room temperature and under 365 nm UV light irradiation for 30 s, the sample recovered to its original shape. In addition, as the content of SP increased, the shape recovery time continued to decrease and the photoplasticization-induced shape recovery rate was accelerated (**Table 1**). The photoplasticization effect was strengthened, and the flexibility of the molecular chain increased continuously, leading to the release of internal storage stress within the temporary shape, and the shape recovery rate was accelerated. We also tested the shape memory process of a "box". After irradiation with 365 nm UV light for 90 s, the "box" was also unfolded, as shown in Figure 4b. In addition, we used SMTPU-SP-0 as an example to test the shape memory process of pure polyurethane, and found that after 365 nm UV light irradiation for 120 s, the temporary shape did not change, as shown in Scheme S2 and Video S1 (Supporting Information). The experiment indirectly proved that the shape recovery behavior of the SMTPU-SP was actuated by the photoplasticization effect, but not by the photothermal effect.

Table 2 lists the shape memory properties of the SMTPU-SP upon 365 nm UV light irradiation for 120 s. The shape fixation ratios of SMTPU-SP-0, SMTPU-SP-1.2, SMTPU-SP-2.4, SMTPU-SP-3.5, and SMTPU-SP-4.6 were 100%, 95.9%, 99.5%, 98.0%, and 97.4%, and the shape recovery ratios were 0%, 84.3%, 90.4%, 90.5%, and 93.7%, respectively. With the increase in SP content, the shape fixation ratio exhibited a downward trend, whereas the shape recovery ratio exhibited an upward trend. With the increase in SP content, the photoplasticization effect was enhanced, which was conducive to the movement of the polyurethane amorphous area and soft segment molecular chains, thereby improving the shape recovery ratio. However, the shape recovery ratio was

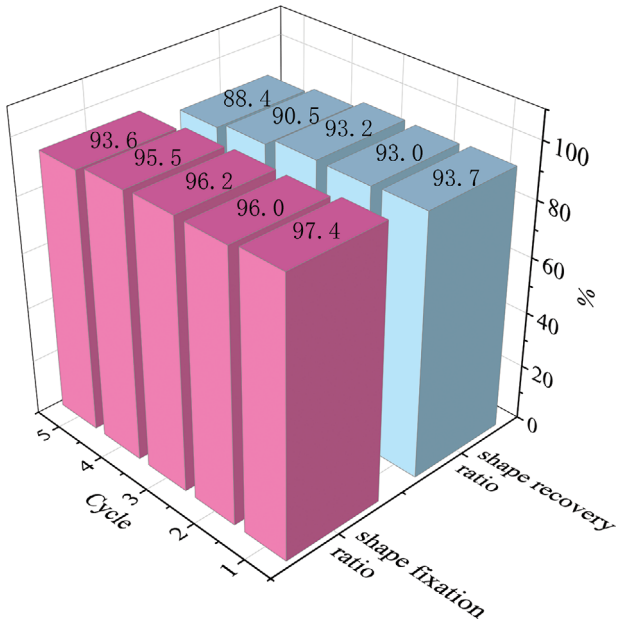

Figure 5. Shape memory properties of SMTPU-SP-4.6 with five cycles.

not 100%. Although the photoplasticization effect of SPs can weaken the interaction force of polyurethane molecular chains, it cannot completely release the internal stress stored in the crystal region of the soft segment; thus, the shape cannot be restored completely. By reheating to a temperature above the melting point of the soft segment, the shape can be restored by 100%.

Taking SMTPU-SP-4.6 as an example, we also tested the shape memory cycle process five times, and the shape fixation and shape recovery ratios are shown in **Figure 5**. The fifth shape fixation and shape recovery ratios were 93.6% and 88.4%, respectively, indicating that the ring-opened and ring-closed structure transitions of the SP molecule were repeatable; however, the shape recovery performance exhibited a downward trend. Because the sample was rapidly reduced from a high-temperature environment to 0 °C, the material was quenched, small crystals were easily formed, and the structural regularity of the soft molecular chain was destroyed, leading to a decrease in crystallinity. After five cycles, the crystallinity of the soft segment continued to decline; therefore, the ability to fix the temporary shape

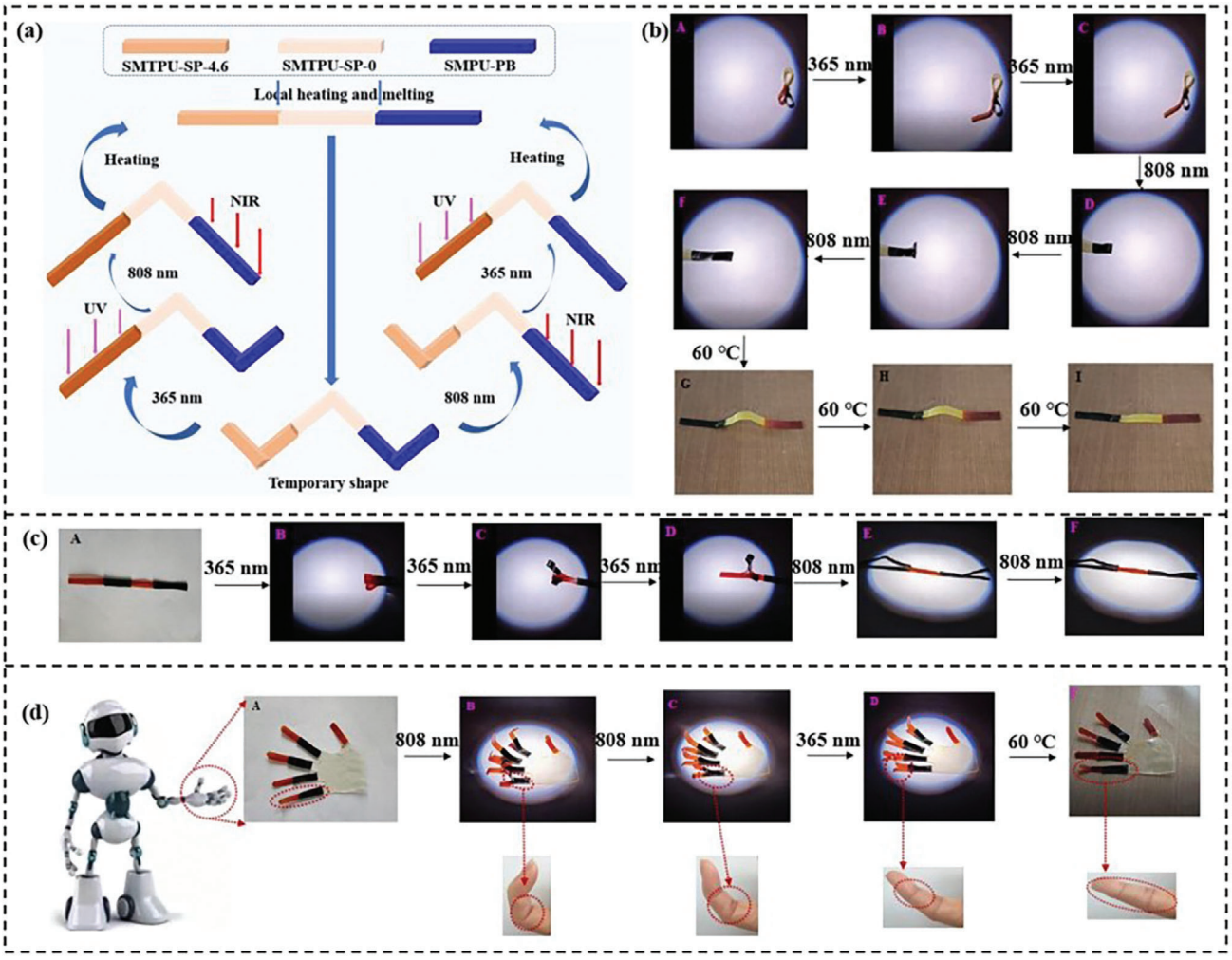

Figure 6. a) Diagram of programmable multi-responsive multi-segments motion, b) photos of the shape recovery processes of SMPUs film under 365 nm UV light, 808 nm NIR light irradiation, and 60 °C thermal field, respectively, c) programmable photo-actuated four-segments shape recovery process under 365 nm UV light and 808 nm NIR light irradiation, d) open process of "bionic finger" under 365 nm UV light, 808 nm NIR light irradiation, and 60 °C thermal field.

dropped. The shape recovery ratio also exhibited a downward trend because in the shape memory process, the ring-closed and ring-opened structure of the SP molecule was continuously converted, that is, it continuously changed between the 2D and three-dimensional structures. After multiple UV light irradiations, the conversion ability of the SP molecule decreased; thus, the shape recovery ratio also decreased.

The programmable multi-responsive multi-segment motion is illustrated in **Figure 6**a. SMTPU-SP-4.6, SMTPU-SP-0, and SMPU-PB were combined into the multi-responsive composites. SMTPU-SP-4.6, SMTPU-SP-0, and SMPU-PB were thermoplastic polymers; therefore, they could be compounded together by local heating and melting, named SMPUs. By controlling the different wavelengths, the shape recovery process was performed in different parts of the SMPUs. If irradiated with 365 nm UV light and 808 nm NIR light in sequence, the temporary shapes of SMTPU-SP-4.6 and SMPU-PB would be restored in sequence. In contrast, if irradiated with 808 nm NIR light and 365 nm UV light in sequence, the temporary shapes of SMPU-PB and SMTPU-SP-4.6 would be restored in sequence. Finally, the SMPUs were heated to temperatures above the shape memory transition temperature, and the segments of the composites all returned to their original shapes. Figure 6b shows the shape recovery process of SMPUs under 365 nm UV light, 808 nm NIR light irradiation, and 60 °C thermal field. First, the SMTPU-SP-4.6 segment was irradiated with 365 nm UV light, which could be unfolded. Then, the SMPU-PB segment was placed under 808 nm NIR light irradiation, and it could also be unfolded. Finally, the SMPU film was placed on a heating platform at 60 °C, and SMTPU-SP-0 was restored from a curved state to a flat state. Videos of multi-responsive multi-segment shape recovery processes are shown in Video 2a–c (Supporting Information).

In addition, we used SMTPU-SP-4.6 and SMPU-PB to manufacture a programmable photo-actuated four-segment composite thin film, as shown in Figure 6c. After 365 nm UV light irradiation, the SMTPU-SP-4.6 segments were partially returned

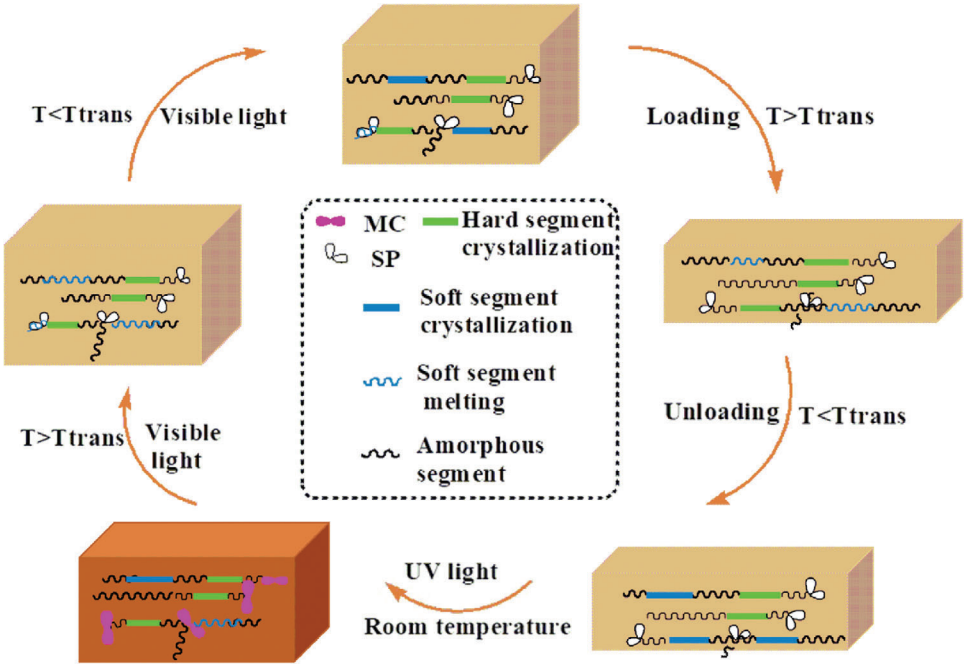

Figure 7. Shape memory mechanism of UV-actuated SMTPU-SP.

to their original shape, and after 808 nm NIR light irradiation, the SMPU-PB segments were returned to their original shape; thus, the shape memory process demonstrated programmable multi-segment movement processes, and had potential applications in programmable soft actuators. Additionally, as shown in Figure 6d, "bionic fingers" were prepared using SMTPU-SP-4.6, SMTPU-SP-0, and SMPU-PB. Among them, Figure 6d-A is the initial shape of "finger open," which was programmed as "bent" state upon external force. After 808 nm NIR light irradiation, the SMPU-PB segment exhibited shape recovery, and the "finger" was partly unfolded. After 365 nm UV light irradiation, the SMTPU-SP-4.6 segment exhibited shape recovery, and the "finger" continued to unfold, but it was not completely unfolded. After heating at 60 °C, the "finger" was completely unfolded. The shape recovery process was in attachment Video 3a–c (Supporting Information).

Figure 7 shows the shape memory mechanism of the UV-actuated SMTPU-SP. Polyurethane has a microphase separation structure comprising soft and hard segments. The soft segments are long chains formed by polyether polyols and have a low transition temperature. The hard segments comprise chain extenders and polyisocyanates, which have a higher transition temperature. In general, the hard and soft segments are thermodynamically incompatible; thus, the polymer exhibits a micro-phase separation phenomenon. Among them, the micro-region of the soft segments plays a role in fixing the temporary shape, that of the hard segments plays the role of maintaining the permanent shape, and the SP plays the role of photoplasticization. When the ambient temperature is higher than the crystalline melting temperature of the soft segments and lower than the crystalline melting temperature of the hard segments, the SMTPU-SP polymer becomes soft, and the polymer can be shaped by an external force. When the temperature drops below the crystalline melting temperature of the soft segments, the soft segments harden accordingly, and the temporary shape can be maintained even if the external force is removed. After irradiation with 365 nm UV light, the C–O bond of the SP molecule is broken, resulting in isomerization to form ring-opened structures and rearrangement of the molecular structure and electron configuration. These ring-opened structures weaken the interaction force of the polymer molecular chains; thus, the molecular chains of the soft segments become soft and move faster, facilitating the restoration of the polymer from a temporary shape to its original shape. However, it cannot completely release the internal stress stored in the crystal region of the soft segments; therefore, the shape cannot be restored completely. By reheating to temperatures above the melting point of the soft segments, the shape can be restored to 100%; then, it can enter the next shape memory cycle.

3. Conclusions

In this study, SMTPU-SP with a shape memory effect, photochromism, and mechanochromism was fabricated by grafting *N*-hydroxyethyl-3,3-dimethyl-6-nitroindoline grafted into a polyurethane matrix. The UV-actuated shape memory performance test revealed that SMTPU-SP-4.6 had the best shape recovery performance, with shape fixation and shape recovery ratios of 97.4% and 93.7%, respectively. In addition, SMTPU-SP was demonstrated to exhibit photochromic and mechanochromic behaviors, which turned purple under 365 nm UV light irradiation or tensile force. Furthermore, multi-segment "bionic fingers" were proven to have multi-selective light-actuated deformation characteristics. It is believed that multifunctional intelligent materials will be used in programmable soft actuators and stress sensors.

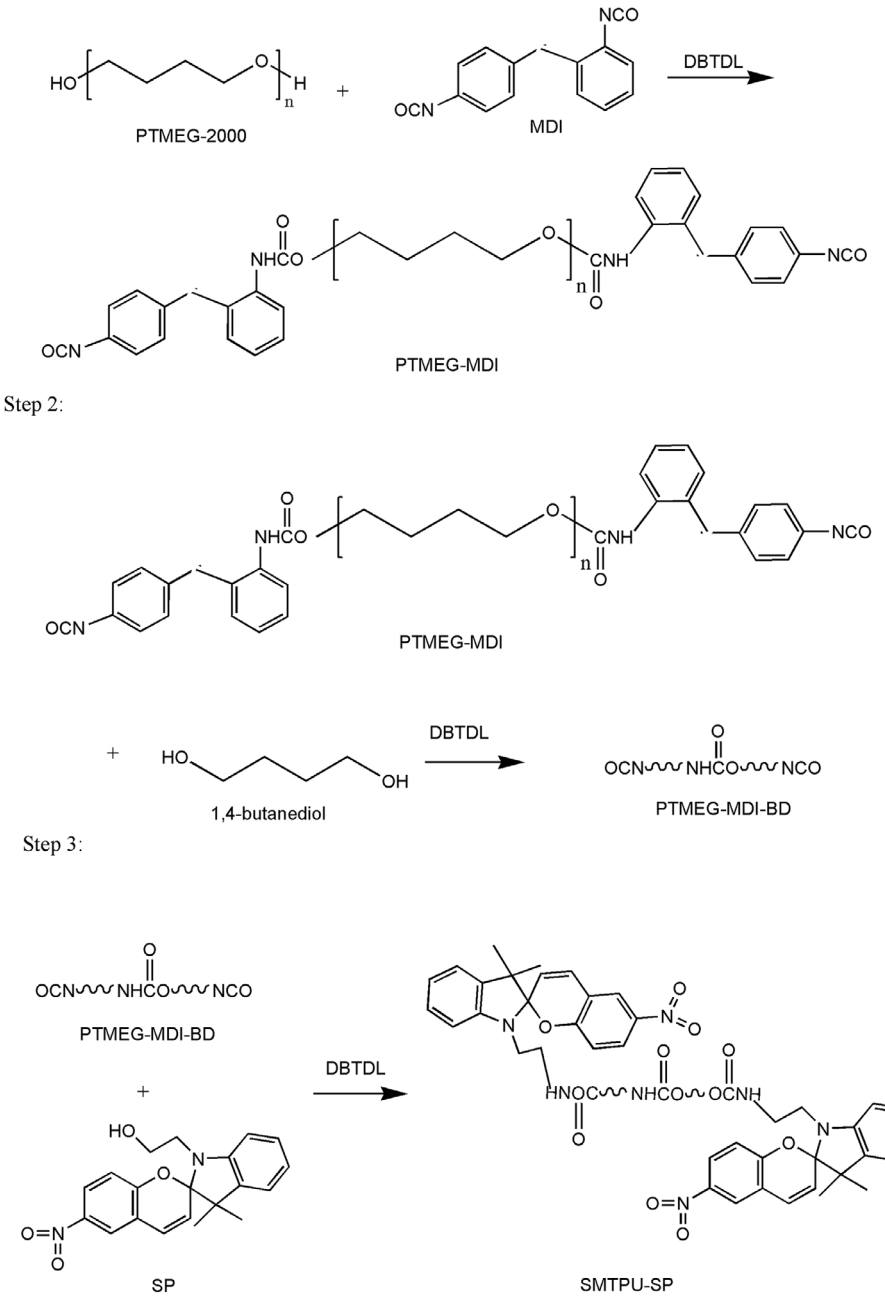

Figure 8. Synthesis route of the SMTPU-SP.

4. Experimental Section

Materials: *N*-hydroxyethyl-3,3-dimethyl-6-nitroindoline SP was obtained from Tianjin Seterui Technology Development Co., Ltd. Diphenylmethane diisocyanate (MDI), polytetrahydrofuran dialcohol (PTMEG-2000, Mn = 2000, removed water at 120 °C for 3 h), 1,4-butanediol, and dibutyltin dilaurate (DBTDL) were purchased from Shanghai Aladdin Reagent Co., Ltd. *N*, *N*-dimethylformamide (DMF), which was analytically pure, was obtained from Tianjin Fengchuan Chemical Reagent Technology Co., Ltd. SMPU-PB was obtained from the laboratory, which had shape deformation upon 808 nm NIR light irradiation, and the preparation of SMPU-PB is shown in the Supporting Information.

Preparation of SP Graft SMPU: a) At room temperature, PTMEG-2000 and DMF were added to the dry three-necked flask. Then, MDI was dropped in the system within 5 min during which the molar ratio of PTMEG-2000 to MDI was 1: 3, and 0.5 wt% DBTDL was added to the system after stirring for 15 min. Next, the system was heated to 60 °C and allowed to react for 1 h. In this step, an isocyanate-terminated polyurethane prepolymer, named PTMEG-MDI, was fabricated. The reaction is shown in **Figure 8** (step 1).

b) Different molar amounts of 1,4-butanediol (BD) were added to the PTMEG-MDI system, and the molar ratios of PTMEG-MDI to BD were 2:1.80, 2:1.85, 2:1.90, 2:1.95, and 2:2, respectively. The system was then allowed to react for 1 h at 60 °C. In this step, a hydroxyl-terminated

polyurethane prepolymer, named PTMEG-MDI-BD, was fabricated. The reaction is shown in Figure 8 (step 2).

c) N-hydroxyethyl-3,3-dimethyl-6-nitroindoline SP with different molar amounts was added to the PTMEG-MDI-BD system, with molar ratios of 0.2:0.4, 0.15:0.3, 0.1:0.2, 0.05:0.1, and 0:0, respectively. The reaction was allowed to proceed for 2 h at 60 °C. Thereafter, the system was poured into a polytetrafluoroethylene mold and stored at 80 °C in a vacuum box until the DMF solvent in the polyurethane was completely volatilized. The SMPUs with SP content were 4.6, 3.5, 2.4, 1.2, and 0 wt%, named SMTPU-SP-4.6, SMTPU-SP-3.5, SMTPU-SP-2.4, SMTPU-SP-1.2, and SMTPU-SP-0, respectively. The reaction is shown in Figure 8 (step 3).

Preparation of Multi-Stimuli and Multi-Segment Shape Memory Composites: SMTPU-SP-4.6, SMTPU-SP-0, and SMPU-PB were spliced together in sequence, with an overlap length of 5 mm. Using the method of local heating and melting, the thin film was locally heated to a viscous flow state, and the three sections were bonded together to prepare multi-segment shape memory composites, named SMPUs (see Scheme S3, Supporting Information).

Characterization: The molecular structure of SMTPU-SP was tested using an AVATAR360 spectrometer (FTIR) and ^{1}H NMR (solvent was $CDCl_3$). The molecular structure of the SP before and after UV irradiation and before and after stress was tested using a Daojin UV-3600 UV–vis spectrophotometer. WAXD was used to study the crystallization of SMTPU-SP before and after UV irradiation. The SAXS test was performed on the SMTPU-SP using the Shanghai Synchrotron Radiation Device (SSRF) BL16B1 line station. The glass transition temperature of the SMTPU-SP was tested using a Mettler Toledo DSC1 differential scanning calorimeter. The thermal stability of the SMTPU-SP was tested using a DSC1 synchronous thermal analyzer (METTLER-TOLEDO Corporation, Switzerland). The dynamic thermomechanical performance of the SMTPU-SP was tested by a dynamic mechanical analyzer DMA Q800 (TA Corporation, USA). The results are shown in Scheme S5 (Supporting Information).

Characterization of Photochromic and Mechanochromic Effects: The SMTPU-SP was irradiated with 365 nm UV light with an intensity of 1.5 mW cm^{-2} for 10 s, and its color was observed. The photochromic saturation time of the SMTPU-SP upon 365 nm UV light irradiation, and the photochromic recovery time upon visible light irradiation (1.5 mW cm^{-2}) to determine the ring-opened and ring-closed transition rates were also tested. In addition, the sample was stressed by a microcomputer tensile testing machine SBA-10 (Chongqing Haco Technology Co., Ltd.), and its color was observed.

Qualitative Characterization of Photo-Actuated Shape Memory Performance: The SMTPU-SP was heated to 60 °C for 10 min, bent in half, and subsequently cooled to 0 °C under external force for 10 min to fix the temporary shape. Finally, the sample was irradiated with 365 nm UV light (1.5 mW cm^{-2}, Beijing Newbit Technology Co., Ltd.) to achieve the macro photo-actuated shape recovery process.

Quantitative characterization: The shape fixation process was the same as described above, and the sample was irradiated with 365 nm UV light (Beijing Newbit Technology Co., Ltd.) for 120 s to measure the shape recovery ratio. The shape memory cycle process was tested five times, and the shape fixation and shape recovery ratios are shown in Scheme S4 (Supporting Information).

Supporting Information

Supporting Information is available from the Wiley Online Library or from the author.

Acknowledgements

This work was supported by the National Natural Science Foundation of China (Grant Nos. 11632005 and 11802077) and Heilongjiang Touyan Innovation Team Program. The authors thank the staff from BL19U2 beamline of National Facility for Protein Science in Shanghai (NFPS) at Shanghai Synchrotron Radiation Facility, for assistance during data collection.

Conflict of Interest

The authors declare no conflict of interest.

Data Availability Statement

Data available on request from the authors. The data that support the findings of this study are available from the corresponding author upon reasonable request.

Keywords

mechanochromic effects, photo-actuated shape memory polyurethane, photochromic effects, programmable soft actuators, spiropyran

Received: October 18, 2021
Revised: December 30, 2021
Published online:

[1] P. K. Panda, J.-M. Yang, Y.-H. Chang, *Carbohydr. Polym.* **2021**, *257*, 117633.
[2] F. Li, L. Liu, L. Du, Y. Liu, J. Leng, *Compos. Struct.* **2020**, *242*, 112196.
[3] T. Koga, K. Tomimori, N. Higashi, *Macromol. Rapid Commun.* **2020**, *41*, 1900650.
[4] H. Chu, X. Hu, Z. Wang, J. Mu, N. Li, X. Zhou, S. Fang, C. S. Haines, J. W. Park, S. Qin, N. Yuan, J. Xu, S. Tawfick, H. Kim, P. Conlin, M. Cho, K. Cho, J. Oh, S. Nielsen, K. A. Alberto, J. M. Razal, J. Foroughi, G. M. Spinks, S. J. Kim, J. Ding, J. Leng, R. H. Baughman, *Science* **2021**, *371*, 494.
[5] G. Li, Y. P. Wang, S. W. Wang, Z. T. Liu, Z. W. Liu, J. Q. Jiang, *Macromol. Mater. Eng.* **2019**, *304*, 1800603.
[6] Y. Xia, Y. He, F. Zhang, Y. Liu, J. Leng, *Adv. Mater.* **2021**, *33*, 2000713.
[7] T. Tian, J. Wang, S. S. Wu, Z. J. Shao, T. Xiang, S. B. Zhou, *Polym. Chem.* **2019**, *10*, 3488.
[8] E. D'Elia, H. S. Ahmed, E. Feilden, E. Saiz, *Appl. Mater. Today* **2019**, *15*, 185.
[9] W. X. Wang, D. Y. Liu, Y. J. Liu, J. S. Leng, D. Bhattacharyya, *Compos. Sci. Technol.* **2015**, *106*, 20.
[10] R. Tonndorf, D. Aibibu, C. Cherif, *Polymers* **2020**, *12*, 2989.
[11] L. K. Jang, G. K. Fletcher, M. B. B. Monroe, D. J. Maitland, *J. Biomed. Mater. Res., Part A* **2020**, *108*, 1281.
[12] X. He, Y. Sun, J. Wu, Y. Wang, F. Chen, P. Fan, M. Zhong, S. Xiao, D. Zhang, J. Yang, J. Zheng, *J. Mater. Chem. C* **2019**, *7*, 4970.
[13] J. Q. Xiong, H. S. Luo, D. C. Gao, X. R. Zhou, P. Cui, G. Thangavel, K. Parida, P. S. Lee, *Nano Energy* **2019**, *61*, 584.
[14] L. Xia, M. Zhang, H. Gao, G. X. Qiu, Z. X. Xin, W. X. Fu, *Polym. Test.* **2019**, *81*, 106212.
[15] W. B. Kuang, P. T. Mather, *J. Mater. Res.* **2018**, *33*, 2463.
[16] N. Zheng, G. Q. Fang, Z. L. Cao, Q. Zhao, T. Xie, *Polym. Chem.* **2015**, *6*, 3046.
[17] Z. L. Zhang, J. Du, W. W. Shan, T. B. Ren, Z. Lu, *Macromol. Mater. Eng.* **2020**, *306*, 2000508.
[18] Z. T. Zhou, Y. Meng, C. Wei, Y. Bai, X. Y. Wang, D. P. Quan, J. Zhou, *Macromol. Mater. Eng.* **2021**, *306*, 2100254.
[19] X. Wan, F. H. Zhang, Y. J. Liu, J. S. Leng, *Carbon* **2019**, *155*, 77.
[20] S. S. Wu, Z. J. Shao, H. Xie, T. Xiang, S. B. Zhou, *J. Mater. Chem. A* **2021**, *9*, 1048.
[21] Z. Li, X. Zhang, S. Wang, Y. Yang, B. Qin, K. Wang, T. Xie, Y. Wei, Y. Ji, *Chem. Sci.* **2016**, *7*, 4741.
[22] R. Tonndorf, M. Kirsten, R. D. Hund, C. Cherif, *Text. Res. J.* **2015**, *85*, 1305.

[23] Y. Li, M. Goswami, Y. Zhang, T. Liu, J. Zhang, M. R. Kessler, L. Wang, O. Rios, *Sci. Rep.* **2020**, *10*, 20214.
[24] R. Liu, Q. Zhang, Q. Zhou, P. Zhang, H. Dai, *J. Mech. Behav. Biomed. Mater.* **2018**, *82*, 9.
[25] C. Meiorin, D. G. Actis, F. E. Montoro, O. M. Londoño, M. I. Aranguren, D. Muraca, P. M. Zélis, M. Knobel, M. A. Mosiewicki, *Phys. Status Solidi A* **2018**, *215*, 1800311.
[26] Y.-Y. Xiao, X.-L. Gong, Y. Kang, Z.-C. Jiang, S. Zhang, B.-J. Li, *Chem. Commun.* **2016**, *52*, 10609.
[27] L. X. Lu, T. Tian, S. S. Wu, T. Xiang, S. B. Zhou, *Polym. Chem.* **2019**, *10*, 1920.
[28] T. Tian, J. Wang, S. S. Wu, Z. J. Shao, T. Xiang, S. B. Zhou, *Polym. Chem.* **2019**, *10*, 3488.
[29] H. Venkatesan, J. M. Chen, H. Y. Liu, Y. Kim, S. Na, W. Liu, J. L. Hu, *Mater. Chem. Front.* **2019**, *3*, 2472.
[30] A. S. Kuenstler, K. D. Clark, J. R. De Alaniz, R. C. Hayward, *ACS Macro Lett.* **2020**, *9*, 902.
[31] B. G. Peng, Y. C. Yang, K. Gu, E. J. Amis, K. A. Cavicchi, *ACS Mater. Lett.* **2019**, *1*, 410.
[32] X. H. Huang, F. N. Xu, H. B. Hou, J. W. Hou, Y. Wang, S. B. Zhou, *Nano Res.* **2019**, *12*, 1361.
[33] Q. Guo, C. J. Bishop, R. A. Meyer, D. R. Wilson, L. Olasov, D. E. Schlesinger, P. T. Mather, J. B. Spicer, J. H. Elisseeff, J. J. Green, *ACS Appl. Mater. Interfaces* **2018**, *10*, 13333.
[34] X. Pang, J.-A. Lv, C. Zhu, L. Qin, Y. Yu, *Adv. Mater.* **2019**, *31*, 1904224.
[35] R. Yan, B. X. Jin, Y. J. Luo, X. Y. Li, *Polym. Chem.* **2019**, *10*, 2247.
[36] A. Lendlein, H. Jiang, O. Jünger, R. Langer, *Nature* **2005**, *434*, 879.
[37] P. Zhang, B. Wu, S. Huang, F. Cai, G. Wang, H. Yu, *Polymer* **2019**, *178*, 121644.
[38] H. J. Guo, H. Jin, R. J. Gui, Z. H. Wang, J. F. Xia, F. F. Zhang, *Sensor. Actuat. B-Chem.* **2017**, *253*, 50.
[39] S. Chen, Y. J. Gao, Z. Q. Cao, B. Wu, L. Wang, H. Wang, Z. M. Dang, G. J. Wang, *Macromolecules* **2016**, *49*, 7490.
[40] Q. Zhang, D. H. Qu, H. Tian, *Adv. Opt. Mater.* **2019**, *7*, 1900033.
[41] Z. L. Wu, Z. J. Wang, P. Keller, Q. Zheng, *Macromol. Rapid Commun.* **2016**, *37*, 311.
[42] Y. K. Bai, J. W. Zhang, D. D. Wen, P. W. Gong, X. Chen, *Compos. Sci. Technol.* **2019**, *170*, 101.
[43] X. Zhang, Q. Zhou, H. Liu, H. Liu, *Soft Matter* **2014**, *10*, 3748.
[44] E. Samoylova, L. Ceseracciu, M. Allione, A. Diaspro, A. C. Barone, A. Athanassiou, *Appl. Phys. Lett.* **2011**, *99*, 201905.
[45] H. M. Dou, J. H. Ding, H. Chen, Z. Wang, A. F. Zhang, H. B. Yu, *RSC Adv.* **2019**, *9*, 13104.
[46] Y. Kawabe, K. Okoshi, *Opt. Mater. Express* **2018**, *8*, 332.
[47] W. Qiu, P. A. Gurr, G. G. Qiao, *ACS Appl. Mater. Interfaces* **2019**, *11*, 29268.
[48] Z. Q. Cao, *Macromol. Chem. Phys.* **2020**, *221*, 2000190.
[49] Y. Chen, C. J. Yeh, Y. Qi, R. Long, C. Creton, *Sci. Adv.* **2020**, *6*, 5093.
[50] D. A. Davis, A. Hamilton, J. Yang, L. D. Cremar, D. Van Gough, S. L. Potisek, M. T. Ong, P. V. Braun, T. J. Martínez, S. R. White, J. S. Moore, N. R. Sottos, *Nature* **2009**, *459*, 68.